



Therapeutic inhibition of MPO stabilizes pre-existing high risk atherosclerotic plaque

Weiyu Chen^{a,b,1}, Sergey Tumanov^{a,b,1}, Stephanie M.Y. Kong^a, David Cheng^c, Erik Michaëlsson^d, André Bongers^e, Carl Power^e, Anita Ayer^a, Roland Stocker^{a,f,*}

^a Heart Research Institute, The University of Sydney, Sydney, Australia

^b Faculty of Medicine and Health, The University of Sydney, Sydney, Australia

^c Victor Chang Cardiac Research Institute, Sydney, Australia

^d Early Clinical Development, Research and Early Development, Cardiovascular, Renal and Metabolism, BioPharmaceuticals R&D, AstraZeneca, Gothenburg, Sweden

^e Biological Resources Imaging Laboratory, University of New South Wales, Sydney Australia

^f School of Life and Environmental Sciences, The University of Sydney, Sydney, Australia

ARTICLE INFO

Keywords:

Atherosclerosis
Unstable plaque
Myeloperoxidase (MPO)
Myeloperoxidase inhibitor
AZM198
Magnetic resonance imaging (MRI)
MPO-Gd

ABSTRACT

Currently there are no established therapies to treat high-risk patients with unstable atherosclerotic lesions that are prone to rupture and can result in thrombosis, abrupt arterial occlusion, and a precipitous infarction. Rather than being stenotic, rupture-prone non-occlusive plaques are commonly enriched with inflammatory cells and have a thin fibrous cap. We reported previously that inhibition of the pro-inflammatory enzyme myeloperoxidase (MPO) with the suicide inhibitor AZM198 prevents formation of unstable plaque in the Tandem Stenosis (TS) mouse model of plaque instability. However, in our previous study AZM198 was administered to animals *before* unstable plaque was present and hence it did not test the significant unmet clinical need present in high-risk patients with vulnerable atherosclerosis. In the present study we therefore asked whether pharmacological inhibition of MPO with AZM198 can stabilize pre-existing unstable lesions in an interventional setting using the mouse model of plaque instability. *In vivo* molecular magnetic resonance imaging of arterial MPO activity using *bis*-5-hydroxytryptamide-DTPA-Gd and histological analyses revealed that arterial MPO activity was elevated one week after TS surgery, prior to the presence of unstable lesions observed two weeks after TS surgery. Animals with pre-existing unstable plaque were treated with AZM198 for one or five weeks. Both short- and long-term intervention effectively inhibited arterial MPO activity and increased fibrous cap thickness, indicative of a more stable plaque phenotype. Plaque stabilization was observed without AZM198 affecting the arterial content of Ly6B.2⁺ and CD68⁺-cells and MPO protein. These findings demonstrate that inhibition of arterial MPO activity converts unstable into stable atherosclerotic lesions in a preclinical model of plaque instability and highlight the potential therapeutic potency of MPO inhibition for the management of high-risk patients and the development of novel protective strategies against cardiovascular diseases.

1. Introduction

Inflammation is now generally recognized to regulate atherosclerotic plaque biology and to contribute to plaque destabilization [1]. The pro-inflammatory enzyme myeloperoxidase (MPO) generates the highly reactive hypochlorite that contributes to the innate immune response against phagocytosed pathogens. However, up to 30% of cellular MPO can be released into the extracellular space [2,3], where the enzyme could cause deleterious oxidative tissue injury which has been linked to

atherogenesis, plaque destabilization, erosion, and rupture [4–6]. Reflecting this, immunohistochemical studies reported more than 20 years ago identified MPO-expressing immune cells and hypochlorite-modified proteins in ruptured and eroded plaques as well as atheromatous lesions of humans [7–9]. Despite this, a key gap in this field is the lack of direct and quantitative information on the role(s) of intraplaque MPO activity in human atherogenesis and plaque stability.

Attempts to clarify the role of MPO in atherogenesis by using pre-clinical models of atherosclerosis have yielded ambiguous results. Using

* Corresponding author. Heart Research Institute, 7 Eliza Street, Newtown, 2042, New South Wales, Australia.

E-mail address: roland.stocker@hri.org.au (R. Stocker).

¹ These authors contributed equally.

a pharmacological approach, Buckbinder and co-workers reported a non-significant increase in lesion area in *Ldlr*^{-/-} mice treated with the MPO inhibitor PF-06282999 versus control [10]. However, treatment with PF-06282999 was associated with a significant decrease in necrotic core area, leading the authors to conclude that MPO inhibition in mice alters atherosclerotic lesion composition [10]. However, PF-06282999 also significantly decreased the lesion content of MPO protein and the homing of CD68⁺-cells (macrophages) to the plaque [10], so that the observed change in lesion composition cannot be ascribed unambiguously to MPO inhibition. An early, substantive study reported transfer of bone marrow-derived cells from *Mpo*^{-/-} mice into irradiated low density lipoprotein receptor-deficient (*Ldlr*^{-/-}) mice to significantly increase atherosclerosis compared with transfer of wildtype bone marrow cells [11]. This unexpected result was observed without changes to white blood cell counts and lipoprotein profiles [11]. The same study also reported a non-significant increase in atherosclerotic lesion areas in *Ldlr*^{-/-} *Mpo*^{-/-} compared with *Ldlr*^{-/-} *Mpo*^{+/+} mice, and concluded that MPO and MPO-derived reactive intermediates protect against rather than promote atherosclerosis in mice [11].

Contrary to Brennan et al. [11], repopulation of irradiated apolipoprotein E gene-deficient (*ApoE*^{-/-}) mice with bone marrow-derived cells from *Mpo*^{-/-} mice was reported to significantly decrease atherosclerosis compared with wildtype bone marrow cell transfer [12]. The same study also reported high concentrations of 4-aminobenzoic acid hydrazide (4-ABAH, MPO inhibitor) to decrease atherosclerosis. However, both experimental approaches used by Tiyerili et al. [12] to assess the role of MPO in the pathogenesis of atherogenesis have major limitations. First, the transplantation experiments used did not employ enough bone marrow cells or adequate time for their engraftment and did not verify successful engraftment. Second, 4-ABAH is neither a specific (see, e.g., Ref. [13]) nor an effective MPO inhibitor under biological conditions [14]. Moreover, the decrease in atherosclerotic lesion size was observed in conjunction with a decrease in systemic inflammation [12], that cannot be ascribed to MPO blockade. Together, the above studies indicate that MPO blockade, at best, marginally decreases atherosclerotic lesion size in *Ldlr*^{-/-} and *ApoE*^{-/-} mice.

The standard *Ldlr*^{-/-} and *ApoE*^{-/-} mouse models of atherosclerosis were developed with a focus on lesion size as the major outcome measured. However, its equivalent in clinical cardiology, *i.e.*, the degree of stenosis, is not the only parameter that precipitates an acute myocardial infarction. Indeed, a significant proportion of acute myocardial infarcts are caused by abrupt arterial occlusion as a result of plaque destabilization through rupture, fissuring or endothelial cell erosion rather than stenosis determined by plaque size [15]. As MPO and hypochlorite-modified proteins are present in ruptured plaques of humans [9], we therefore considered the possibility that MPO may play an important role in plaque destabilization rather than atherogenesis *per se* [16]. Because standard *Ldlr*^{-/-} and *ApoE*^{-/-} mice do not form unstable plaques reliably, we instead exploited the recent advent of a mouse model of plaque instability [17]. We observed that in that model, MPO activity was higher in unstable than stable plaque, and that genetic or pharmacological blockade of MPO activity attenuated the formation of unstable plaque [18]. Importantly, the MPO suicide inhibitor used (AZM198) [19,20] decreased plaque MPO activity and plaque instability without affecting circulating leukocytes and lipids, lesion macrophages, MPO protein and lipids [18]. These findings raise the possibility of stabilizing vulnerable plaque via the therapeutic inhibition of arterial MPO activity.

Currently there are no established methods to treat high-risk patients with existing unstable plaques, *i.e.*, vulnerable atherosclerosis. This significant clinical issue was not tested in our previous prevention study as AZM198 was administered to animals *before* unstable plaque was present [18]. In the present study we therefore asked whether inhibition of MPO with AZM198 can stabilize pre-existing unstable lesions in an interventional setting using the mouse model of plaque instability. In doing so, we also asked whether short-term pharmacological inhibition

of MPO could be effective in stabilizing plaque, since there are concerns with long-term anti-inflammatory treatment in the management of high-risk cardiovascular patients [21–24]. We observed that inhibition of arterial MPO activity using AZM198 *after* unstable plaque had formed, stabilized such plaque without affecting arterial infiltration by inflammatory cells or plaque content of MPO protein, irrespective of whether the MPO inhibitor was given for one or five weeks. This is the first demonstration that pharmacological inhibition of MPO activity can stabilize pre-existing vulnerable plaque in a pre-clinical model of plaque instability. Our findings warrant further investigations into the clinical potential of MPO as a therapeutic target for the treatment of patients with high-risk atherosclerosis and residual inflammation.

2. Materials and methods

2.1. Animals

The tandem stenosis (TS) model of plaque instability was used throughout. The TS model provides a unique tool to study plaque that closely resembles unstable, vulnerable human lesions within a defined vessel segment. C57BL/6J male *ApoE*^{-/-} mice were fed a regular chow diet until the age of 6–8 weeks, and then switched to a Western Diet (WD; SF00-219, Specialty Feeds, Western Australia) consisting of 22% fat and 0.15% cholesterol for up to 13 weeks. After 6 weeks of WD, TS surgery was performed by a single operator as described previously [17, 18]. The technique is well tolerated despite significant unstable plaque developing post-TS surgery, as blood can circulate to the brain through the circle of Willis via the left common carotid artery. All procedures were carried out according to the Guidelines for Animal Research of the National Health & Medical Research Council (NHMRC) of Australia as well as the Guide for the Care and Use of Laboratory Animals outlined by the National Institutes of Health (NIH). All animal experiments were approved by the Animal Ethics Committees of the Garvan Institute of Medical Research/St Vincent's Hospital (Protocol 16–33), the University of New South Wales (Protocol 17–162B) and the Sydney Local Health District (Protocol 2020-027).

2.2. Molecular magnetic resonance imaging (MRI)

To assess *in vivo* arterial MPO activity by molecular MRI, animals were anaesthetised with isoflurane (4 and 2%, for induction and maintenance, respectively, with general anesthesia confirmed by pedal reflex) and imaged using a 9.4T Bruker Biospec 94/20 Avance III system (Bruker, Ettlingen, Germany) as described previously [18,25]. Following FLASH time-of-flight (TOF) angiography and T1-weighted fast spin echo (TurboRARE, T1-TSE) acquisition, mice received 0.3 mmol/kg of the MPO molecular sensor *bis*-5-hydroxytryptamide-DTPA-Gd (MPO-Gd) (PeptideSynthetics, Funtley, UK) via tail vein injection and scanned after 60 min using a T1-TSE protocol to examine MPO-Gd entry and retention in tissue. The utility of MPO-Gd has been validated in multiple pre-clinical models [26], including the TS model [18], and MPO-Gd detects MPO activity with higher sensitivity and specificity than assays based on peroxidase activity using 3,3',5,5'-tetramethylbenzidine (TMB) or 10-acetyl-3,7-dihydroxyphenoxazine (ADHP) [27]. Also, MPO-Gd cannot penetrate cells and therefore only detects extracellular MPO, the pool of MPO implicated in plaque destabilization and targeted pharmacologically in this study. Following MRI, animals were returned to their original home cage, allocated diet, and housed until the next MRI scan or euthanized. OsiriX Lite (Pixmeo, Switzerland) software was used for image analysis. To normalize regional grey values from the T1 weighted images, the contrast-to-noise ratio (CNR) was calculated as (Signal Intensity_{vessel wall} – Signal Intensity_{skeletal muscle})/Standard Deviation_{background}. A signal-free region in an image corner was used to determine the signal standard deviation as a measure of background noise. CNR of three consecutive 1 mm slices proximal to the proximal ligature were used to calculate the mean CNR

value. Signal enhancement attributed to MPO-Gd retention and therefore MPO activity was calculated as $\Delta\text{CNR} = \text{CNR}_{\text{post-contrast}} - \text{CNR}_{\text{pre-contrast}}$.

2.3. Intervention study design and AZM198 treatment

Mice were treated with the MPO inhibitor AZM198 for one week (short-term intervention) or five weeks (long-term intervention). Treatment commenced two weeks after TS surgery, i.e., when phenotypically unstable plaque was present as determined in the present

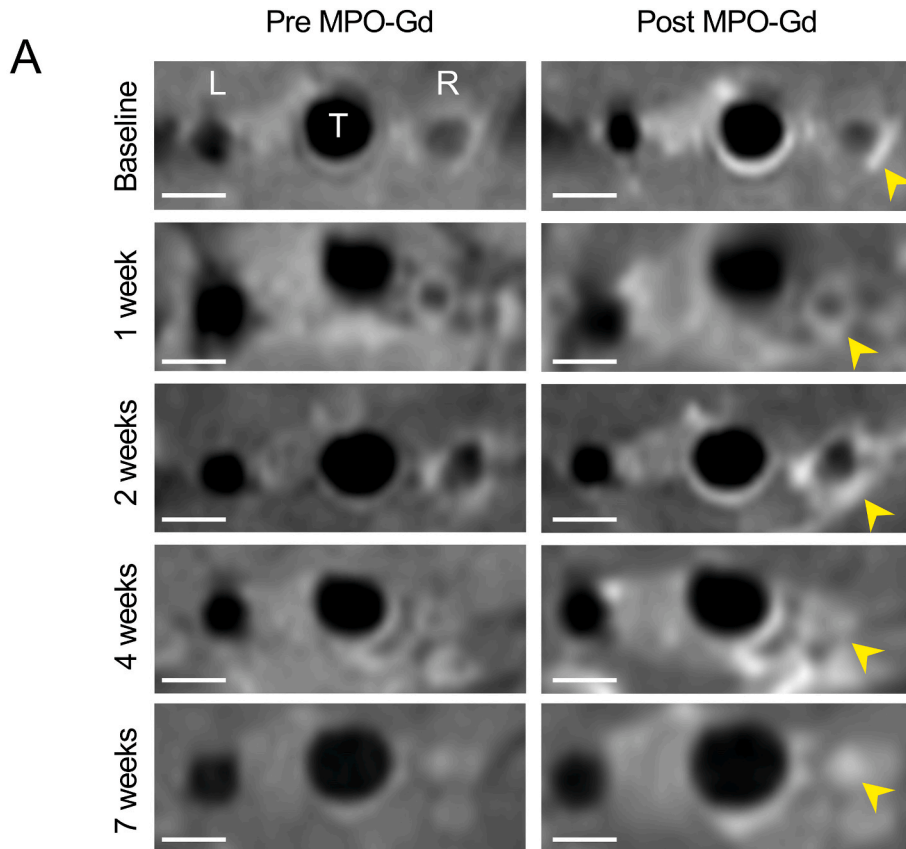
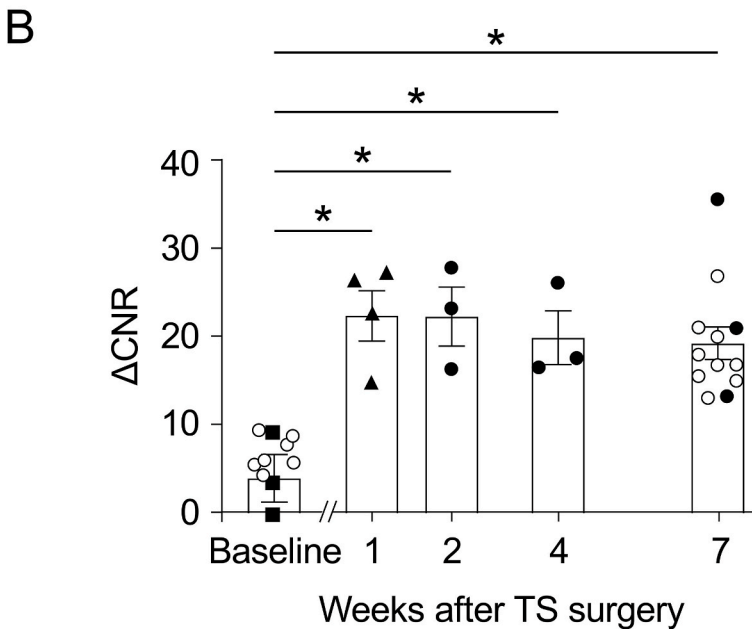


Fig. 1. Arterial MPO activity rapidly and sustainably increases in regions where unstable plaque forms following tandem stenosis (TS) surgery. Arterial MPO activity in unstable plaque was determined by molecular MRI. (A) T1-TSE images of the left (L) plaque-free and right (R) carotid arteries where unstable plaque forms, before and 60 min after administration of MPO-Gd to *ApoE*^{-/-} mice at baseline (before TS surgery) and one, two, four and seven weeks after TS surgery. (B) MPO activity was expressed as ΔCNR ($\text{CNR}_{60} - \text{CNR}_{\text{pre-contrast}}$). A single cohort of animals ($n = 3$, filled circles) was used to assess MPO activity longitudinally at two, four and seven weeks after TS surgery. Separate cohorts of animals were used to assess MPO activity baseline ($n = 3$, filled squares) and one week after TS surgery ($n = 4$, filled triangles), respectively. Open circles at baseline and seven weeks after TS surgery represent previously published data [18]. Each data point represents the mean ΔCNR (60 min post-contrast minus pre-contrast) of 3 consecutive 1 mm slices proximal to the proximal ligation. Data shows mean \pm SEM with $n = 3-9$ animals per group. Significance was evaluated using the Mann-Whitney rank sum test between each experimental group. * $P < 0.05$.



study. Mice received WD containing 500 μmol AZM198 per kg body-weight assuming a daily food consumption of ~ 3.7 g per animal. We reported previously [18] that this dose yields steady state plasma concentrations of AZM198 expected to inhibit extracellular MPO activity by $\sim 90\%$ with limited inhibition of intracellular MPO activity [28]. For the short-term intervention, mice were fed WD fortified with AZM198 between two and three weeks after TS surgery and then returned to drug-free WD for another four weeks. For the long-term intervention, mice were fed WD fortified with AZM198 from two until seven weeks after TS surgery. Untreated animals received standard WD throughout the 13 weeks period and served as controls. Mice were allocated into control, short- and long-term treatment groups in a random order accordingly to the housing cage number to achieve similar numbers per group.

2.4. Blood and tissue collection

Blood (50 μL) was collected from the tail vein two, three, and five weeks after TS surgery for analysis of plasma concentrations of AZM198. At the terminal time point indicated, mice were anaesthetised with isoflurane (4 and 2%, for induction and maintenance, respectively, with general anesthesia confirmed by pedal reflex). Mice were then euthanized by exsanguination through cardiac puncture using a 25-gauge needle and with the blood collected into a heparin-coated tube, centrifuged ($2000\times g$, 15 min, 4 $^{\circ}\text{C}$) and the resulting plasma collected and snap frozen in liquid nitrogen before being stored at -80°C . Animals subsequently were perfused with phosphate-buffered saline and 10% neutral buffered formalin (NBF) solution under physiological pressure. The carotid vascular tree was cleared *in situ* of surrounding connective and adipose tissues, excised, and placed in 10% NBF solution for 16 h then 80% ethanol for further tissue storage. The two tissue collectors were blinded to treatment information.

2.5. Histology

The segment proximal to the proximal ligation of the right carotid artery containing unstable plaque (also referred to as “segment I” [17]) was excised from the vascular tree, dehydrated, paraffin embedded and sectioned using a microtome (RM 2255, Leica Biosystems, Germany), with the two operators blinded to treatment information. The 5 μm sections were then placed on glass slides, deparaffinized, and hydrated. For hematoxylin and eosin (H&E) staining, rehydrated sections were immersed in filtered Mayer’s hematoxylin for 5 min, rinsed with water, then immersed in eosin and stained for 1 min, followed by a 95% (vol/vol) ethanol wash. H&E-stained sections were dehydrated with serial solutions of ethanol and xylene, and then mounted with DPX and sealed with a cover slip. To visualize collagen, the rehydrated tissue sections were stained for 1 h in a solution of picosirius red (PSR), differentiated in 0.01 M HCl, dehydrated with serial solutions of ethanol and xylene, and then mounted with DPX and sealed with a cover slip. To visualize hemosiderin, the rehydrated tissue sections were stained for 30 min in a solution of Perls’ Prussian blue, followed by counterstaining of nuclei with Nuclear Fast Red solution, dehydrated with serial solutions of ethanol and xylene, and then mounted with DPX and sealed with a cover slip. Detailed information of staining reagents is available in Supplementary Table 1.

Immunohistochemistry was performed using a previously described method [29], and antigen retrieval was performed on the rehydrated sections according to the information in Supplementary Table 2. Endogenous peroxidases were quenched with 0.3% (vol/vol) hydrogen peroxide for 20 min. Sections were then blocked with 5% (w/vol) bovine serum albumin, followed by incubation with corresponding primary antibodies or IgG isotype control at 4 $^{\circ}\text{C}$ for 16 h. Detailed information of antibodies is provided in Supplementary Table 2. Sections were incubated with relevant HRP-conjugated secondary antibodies at room temperature for 60 min. After washing with Tris-buffered saline

containing 0.1% (vol/vol) Tween, DAB reagent (K3468, Dako) was applied to each section at room temperature for 10 min and slides washed in distilled water. Sections were then dehydrated and covered with cover slips using DPX mounting media. For representative isotype control images, see Supplementary Fig. 1.

Stained sections were imaged using a Leica Digital Microscope DM4000B-M or Zeiss Axio Scan.Z1 Slide Scanner, and images were analyzed using Image J software (Version 1.49u, NIH, US) by two operators blinded to treatment with treatment information provided by a third person after completion of the analysis. Plaque stability was assessed as described previously [18], using cap thickness as the primary parameter. Briefly, fibrous cap thickness was defined by calculating the positive birefringence area under polarized light in PSR-stained sections. Lesion height was defined by the maximal distance from the lesion to the luminal circumference of the vessel wall in H&E-stained sections [18]. Assessment of positive staining was carried out using Colour Deconvolution 2 Plugin.

2.6. Plasma AZM198 analysis

Plasma (10 μL) was mixed with 990 μL cold (-20°C) acetonitrile/methanol/water (50:30:20, vol/vol/vol), before addition of 10 μL internal standard d_8 -phenylalanine (100 μM DLM-372, Cambridge Isotope Laboratories, USA). AZM198 was analyzed using a previously described untargeted metabolomics mass spectrometry method [30] with d_8 -phenylalanine as the internal standard. The sample was mixed vigorously for 1 min, placed at -20°C for 30 min to precipitate protein and then centrifuged at $17,000\times g$ for 10 min at 4 $^{\circ}\text{C}$. The resulting supernate was collected and freeze-dried, the dried extract dissolved in 100 μL acetonitrile/water (95:5, vol/vol) and the redissolved extract (5 μL) subjected to LC-MS analysis using an Agilent 6560 Q-TOF LC-MS coupled with a 1290 Infinity II UHPLC system. LC-MS parameters were as described previously [30]. AZM198 was detected as $[\text{M}+\text{H}]^+$ ion.

2.7. Statistical analysis

Supplementary Table 3 summarizes the number of animals used for each group in the different experiments. GraphPad Prism 9 software was used for statistical analysis and results expressed as mean \pm SEM. Normality of the data distribution was assessed using D’Agostino-Pearson test and a 1- or 2-way ANOVA, Mann-Whitney, or Kruskal-Wallis test was then used as appropriate for statistical analyses. A *P*-value of <0.05 was considered as statistically significant.

3. Results

3.1. Rapid and sustained increase in arterial MPO activity

We reported previously that seven weeks after tandem stenosis (TS) surgery in *Apoe*^{-/-} mice, MPO activity is higher in unstable compared with stable plaque, and that pharmacological or genetic blockade of MPO prevents formation of unstable plaque [18]. To test whether pharmacological inhibition of MPO can stabilize existing unstable plaque in an intervention setting, we first assessed the time-dependent changes in arterial MPO activity by non-invasive molecular MRI (Fig. 1A) in a cohort of $n = 3$ animals imaged sequentially at two, four and seven weeks after TS surgery (filled circles in Fig. 1B), *i.e.*, time points that allowed assessment of MPO activity across the established seven weeks TS protocol [17,18]. As assessed by the 60 min post-contrast minus pre-contrast ΔCNR value [18], MPO activity was significantly elevated at all three time points. The ΔCNR values obtained were comparable to those published previously for seven weeks after TS surgery (open circles in Fig. 1B) [18], and significantly higher compared with baseline ΔCNR values, determined prior to TS surgery in a separate group of $n = 3$ mice (Fig. 1A, and filled squares in Fig. 1B). As MPO

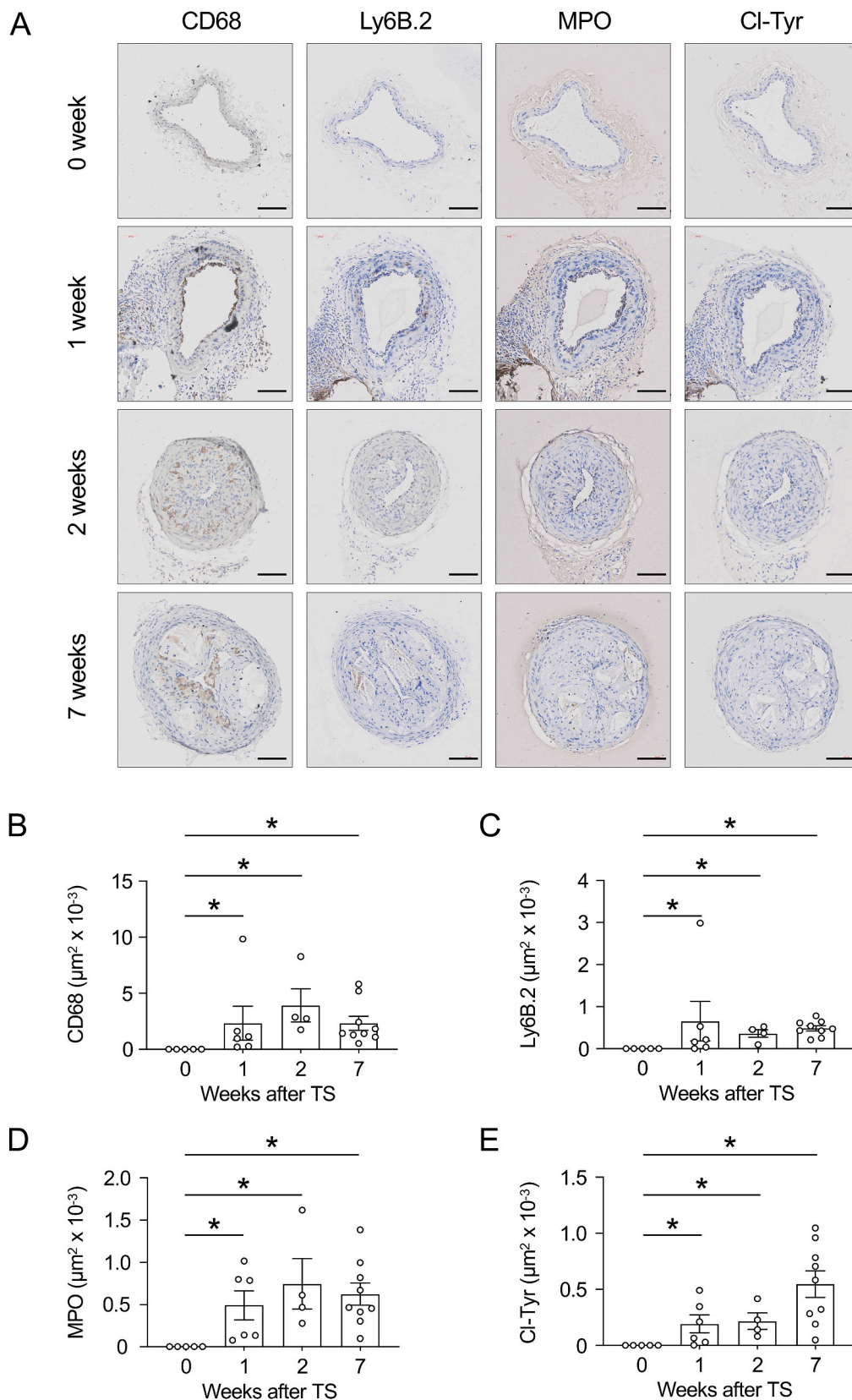


Fig. 2. Inflammatory content of atherosclerotic plaque in the right carotid artery after TS surgery. (A) Representative images of sections of the right carotid artery 0–0.4 mm proximal to the proximal suture obtained immediately after TS surgery (0 week), and one, two and seven weeks after TS surgery, and stained for CD68, Ly6B.2, MPO or chlorotyrosine (Cl-Tyr). Scale bar = 100 µm. (B to E) CD68, Lys6B.2, MPO and Cl-Tyr positive stained area within the 0–0.4 mm region proximal to the proximal suture. Data in B–E show individual values and mean ± SEM with n = 5, 5, 4 and 9 for zero, one, two and seven weeks after TS surgery, respectively. Significance was evaluated using the Mann-Whitney rank sum test between each experimental group. *P < 0.05.

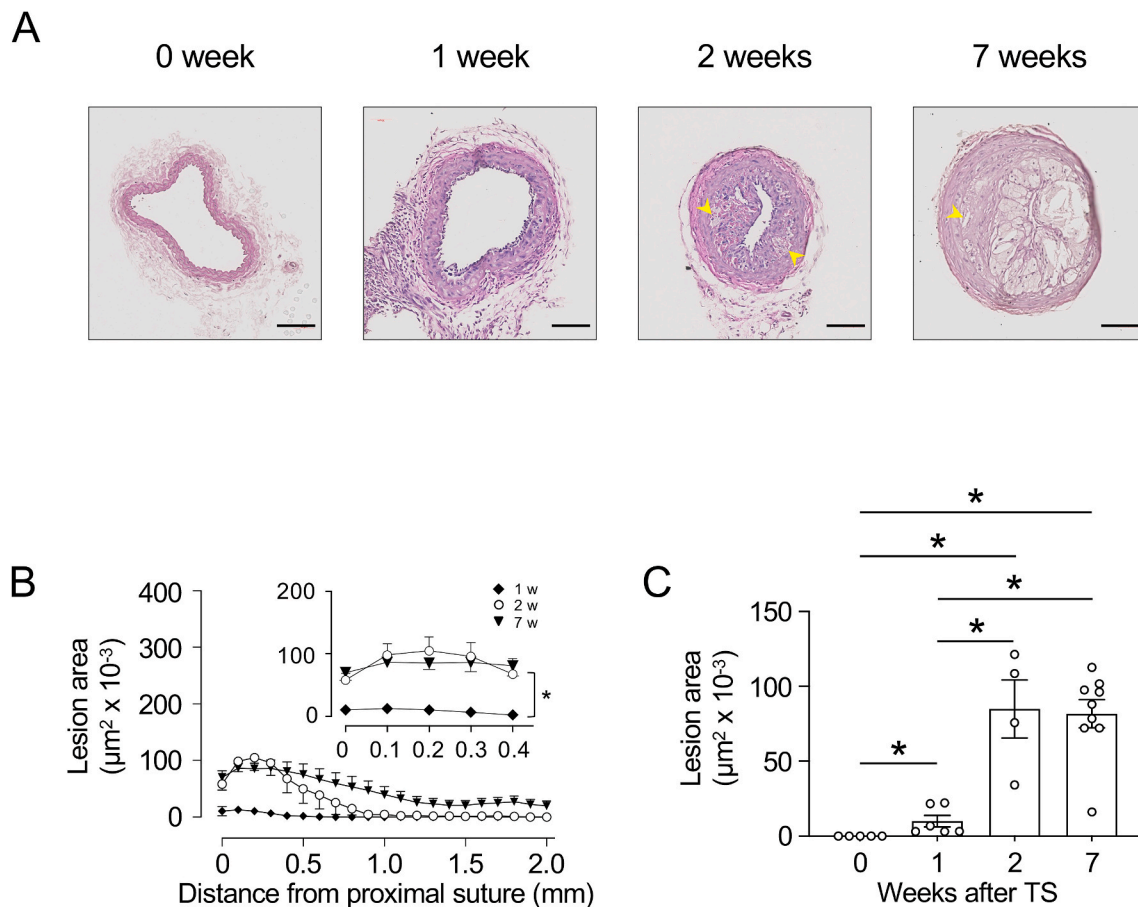


Fig. 3. Atherosclerotic plaque is present two weeks after TS surgery. (A) Representative images of sections of the right carotid artery 0–0.4 mm proximal to the proximal suture stained with H&E. Arrow heads indicate cholesterol clefts. (B) Atherosclerotic lesion area in the 2 mm segment proximal to the proximal suture at one (filled diamonds), two (open circles) and seven weeks (filled triangles) after TS surgery. $*P < 0.01$ as determined by two separate 2-way ANOVA analyses with repeated measures comparing one week with either two or seven weeks after TS surgery. (C) Average atherosclerotic lesion area in the 0–0.4 mm region proximal to the proximal suture. Data in C show individual values as well as mean \pm SEM with $n = 5, 5, 4$ and 9 for zero, one, two and seven weeks after TS surgery, respectively. Significance was evaluated using the Mann-Whitney rank sum test between each experimental group. $*P < 0.05$.

activity was already elevated maximally two weeks after TS surgery, we imaged a third group of $n = 4$ mice one week after TS surgery, the earliest time point that molecular MRI could be carried out following TS surgery. As can be seen (filled triangles in Fig. 1B), MPO activity was significantly elevated at this time point compared with baseline, and indistinguishable from the values observed at two, four and seven weeks after TS surgery (Fig. 1B).

3.2. Arterial infiltration of inflammatory cells is associated with the presence of MPO protein and activity, and precedes the formation of atherosclerotic plaque after TS surgery

As MPO is present in inflammatory cells, we next determined the changes to the arterial content of inflammatory cells, MPO protein and MPO activity after TS surgery. As a control, we included a group of mice (referred to as “0 week”) that were euthanized directly after TS surgery. As expected, at 0 week, arterial segments proximal to the proximal ligature (where unstable plaque forms in this model) were devoid of staining for CD68 (a maker of macrophages), Ly6B.2 (neutrophils), MPO protein and chlorotyrosine (Cl-Tyr; MPO activity [31]) (Fig. 2). However, significant arterial staining of CD68, Ly6B.2, MPO and Cl-Tyr was detected at one week and persisted until seven weeks after TS surgery (Fig. 2), indicating that the arterial infiltration of inflammatory cells was an early event after TS surgery and associated with an increase in both arterial MPO protein and MPO activity. These histological analyses of MPO activity confirmed the molecular MRI results, demonstrating

elevated arterial MPO activity as early as one week after TS surgery.

We next compared the time-dependent increase in arterial inflammation and MPO activity with the appearance of atherosclerosis, as prior to TS surgery plaques are completely absent in the carotid artery where unstable plaques develop (Fig. 3) [17,18]. One week after surgery, atherosclerotic lesions were essentially absent within the 0.4 mm segment proximal to the proximal ligature, as assessed by H&E staining (Fig. 3A). In sharp contrast, at two weeks after TS surgery, lesions were detected with sizes comparable to that seen seven weeks after TS surgery (Fig. 3B–C), as were initial cholesterol clefts (Fig. 3A, Supplementary Fig. 2), although after seven weeks, plaque extended proximally along the artery (Fig. 3B). Together, these findings indicate that arterial infiltration of inflammatory cells and associated presence of MPO protein and activity precede the formation of atherosclerotic plaque in the TS model of plaque instability.

3.3. Presence of unstable plaque two weeks after TS surgery

Next, we determined when unstable plaque first appears in the TS model of plaque instability by histology. The main determinant of plaque stability and its likelihood to rupture is the thickness of its fibrous cap [26]. Therefore, we used cap thickness as the primary parameter to evaluate the appearance of unstable plaque, in addition to the presence of inflammatory cell infiltrate (Fig. 2) and initial cholesterol clefts (Fig. 3A, Supplementary Fig. 2), as well as intraplaque hemorrhage as additional read-outs [26]. Two weeks after TS surgery, lesions showed

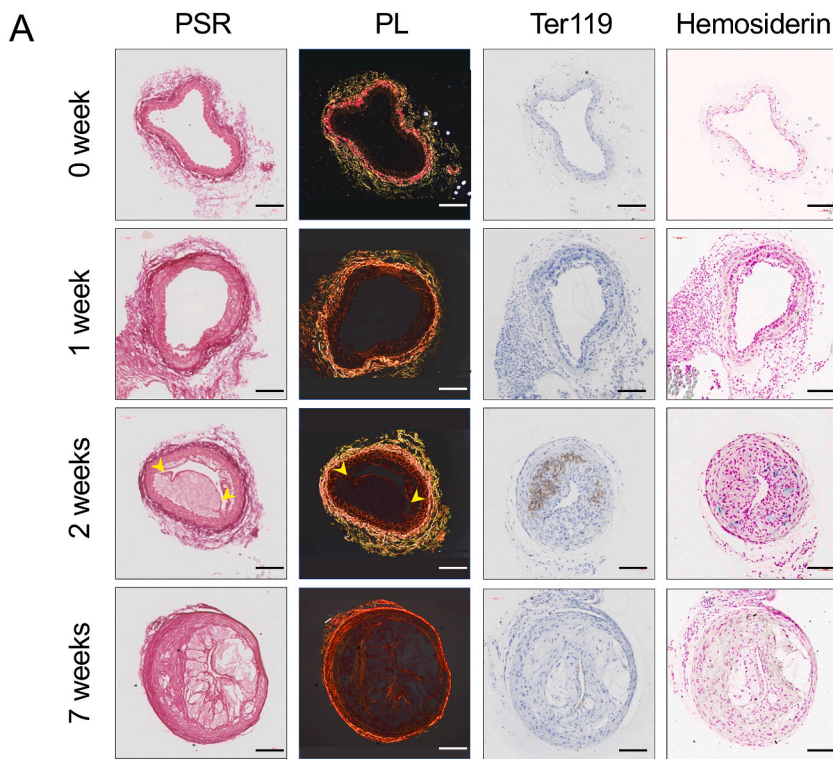
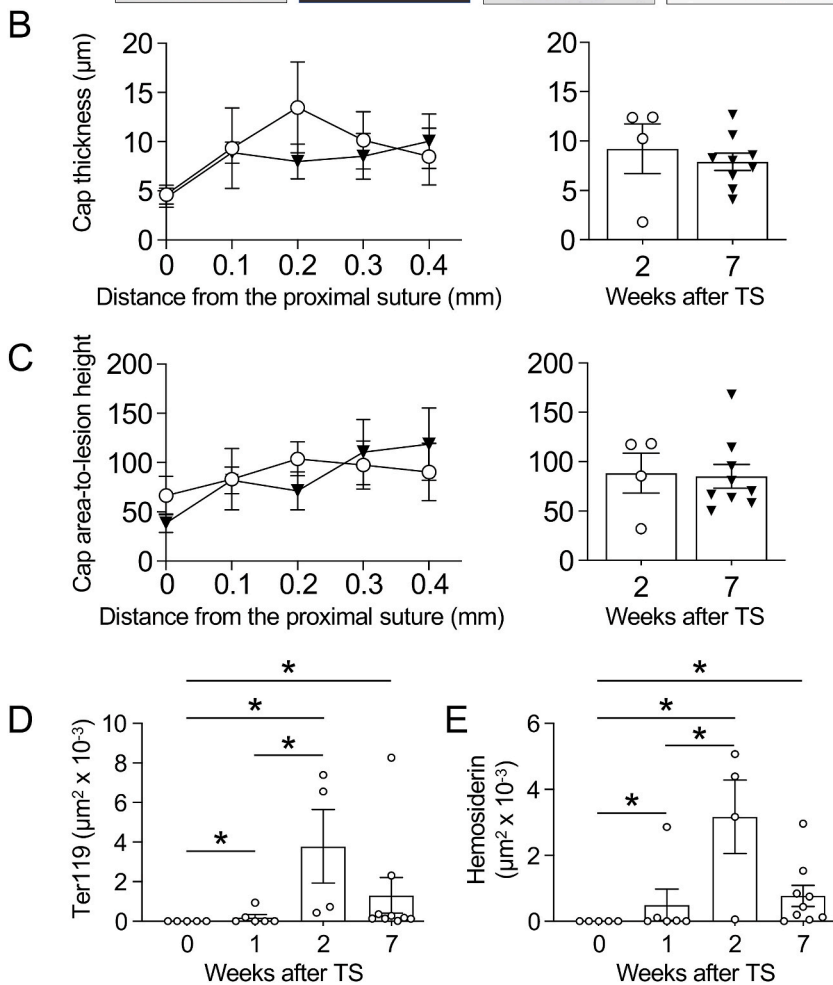
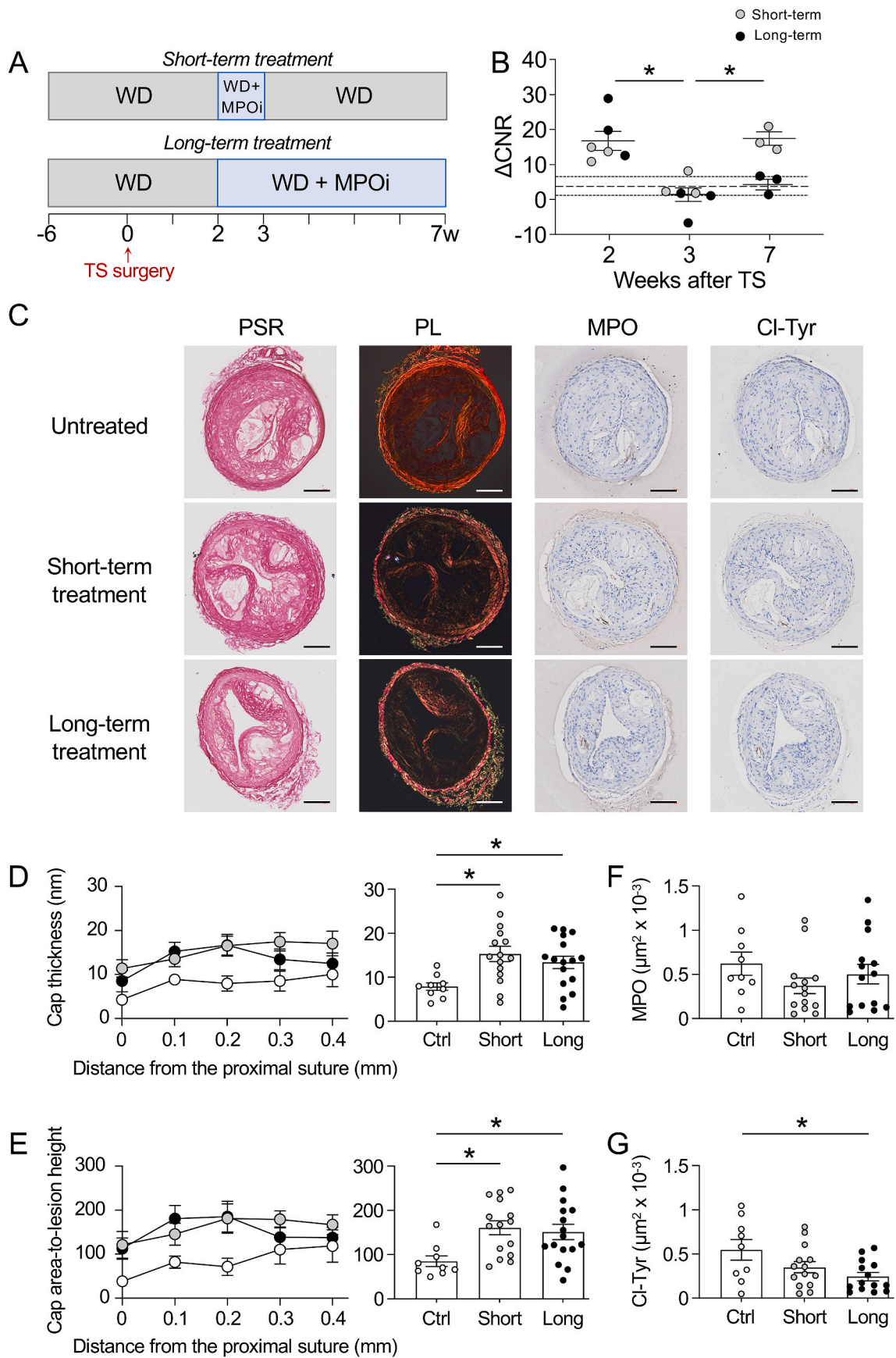


Fig. 4. Atherosclerotic plaque with unstable phenotype is present two weeks after TS surgery, succeeding the increase in arterial MPO activity. (A) Representative images of sections of the right carotid artery 0–0.4 mm proximal to the proximal suture stained with Picrosirius Red (PSR) viewed under bright or polarised light (PL), as well as Ter119 and haemosiderin at zero, one, two and seven weeks after TS surgery. Arrow heads indicate cap thinning at plaque shoulders. Scale bar = 100 μm . Plaque stability was assessed by cap thickness (B) and the cap area-to-lesion height ratio (C) at two (open circles) and seven weeks (filled triangles) after TS surgery. Data shows individual data for the 0–0.4 mm region proximal to the proximal suture (left panels) and respective averages (right panels). (D and E) Average Ter119- and hemosiderin-positive area within the 0–0.4 mm region proximal to the proximal suture. Data shows mean \pm SEM with $n = 5, 5, 4$ and 9 for zero, one, two and seven weeks after TS surgery, respectively. Significance was evaluated using the Mann-Whitney rank sum test between each experimental group. $*P < 0.05$. (For interpretation of the references to colour in this figure legend, the reader is referred to the Web version of this article.)





(caption on next page)

Fig. 5. Pharmacological inhibition of arterial MPO activity stabilizes previously unstable plaque. (A) Schematic representation of the intervention study design. Animals ($n = 6$) were fed Western Diet (WD) for a total of 13 weeks, with TS surgery performed after six weeks of WD. Two weeks after TS surgery, arterial MPO was determined by molecular MRI before mice were placed on WD fortified with the MPO inhibitor AZM198 for one week (short-term) and then re-imaged. The cohort was then divided into two groups, with animals in the short-term treatment arm returned to standard WD until seven weeks after TS surgery. Animals in the long-term MPO inhibition arm continued with WD fortified with AZM198 until seven weeks after TS surgery, *i.e.*, they received the MPO inhibitor for a total of five weeks. Arterial MPO activity was reassessed at the end of the study. (B) MPO activity as measured by molecular MRI in unstable plaque of the short-term (grey circles) and long-term treatment groups (black circles) was expressed as ΔCNR ($\text{CNR}_{60} - \text{CNR}_{\text{pre-contrast}}$). Dashed and dotted lines represent mean \pm SEM of baseline. (C) Representative images of sections of the right carotid artery in region of 0–0.4 mm proximal to the proximal suture obtained from the short- and long-term MPO inhibition groups seven weeks after TS surgery and stained for PSR, PL, MPO or Cl-Tyr. (D to E) Cap thickness and cap area-to-lesion height ratio in the 0–0.4 mm segment proximal to the proximal suture in untreated animals (ctrl, open circles), short-term (grey circles) and long-term MPO inhibition cohorts (black circles) determined seven weeks after TS surgery (left panels), with data also expressed as averages (right panels). (F and G) Average MPO⁺- and Cl-Tyr⁺-stained area within the 0–0.4 mm region proximal to the proximal suture. Data shows mean \pm SEM with $n = 9, 15, 16$ for the untreated, short-term and long-term groups, respectively. Significance was evaluated using the Mann-Whitney rank sum test between each experimental group. * $P < 0.05$.

cap thinning as assessed by picrosirius red (PSR) staining, and signs of intraplaque hemorrhage as assessed by Ter119 and hemosiderin staining (Fig. 4A, Supplementary Fig. 2). These features of unstable plaque were observed in the presence of MPO protein and Cl-Tyr assessed by immunohistochemistry (Supplementary Fig. 2).

Comparison of the lesions in the proximal 0.4 mm segment at two versus seven weeks revealed no significant difference, irrespective of whether cap thickness was assessed itself (Fig. 4B) or expressed as the ratio of cap area-to-lesion height (Fig. 4C). In addition, both measures of intraplaque hemorrhage were observed two weeks after TS surgery, at levels not significantly different to those seen seven weeks after surgery (Fig. 4D–E). Together, these data show that two weeks after TS surgery, unstable plaque is present proximally to the proximal suture as measured by several established indicators of plaque instability, and that its appearance occurs after the increase in arterial MPO activity. Based on these results we concluded that two weeks after TS surgery is a suitable starting point for an intervention study to assess whether pharmacological inhibition of MPO can stabilize established unstable plaque.

3.4. Pharmacological inhibition of arterial MPO activity stabilizes existing unstable plaque

The intervention study was carried out with two experimental arms using the MPO inhibitor AZM198. Drug treatment commenced two weeks after TS surgery, and AZM198 was used at a dose previously shown to preferentially inhibit extracellular MPO and prevent formation of unstable plaque without altering systemic immune functioning, *i.e.*, intragranular MPO activity, circulating leukocytes, cytokines and lipids [18,32]. In the short-term treatment arm, animals received AZM198 for one week (between two and three weeks after surgery, Fig. 5A) and thereafter drug-free WD until seven weeks after TS surgery. In the long-term treatment arm, animals received AZM198 for five weeks (from two to seven weeks after surgery, Fig. 5A).

Molecular MRI using MPO-Gd confirmed that treatment with AZM198 for one and five weeks effectively decreased arterial MPO activity (Fig. 5B) to baseline level (Fig. 1B). In the short treatment arm, arterial MPO activity returned to pre-intervention values by the end of the study (Fig. 5B, open circles), *i.e.*, four weeks after cessation of the drug treatment. Compared with untreated animals (controls), short- and long-term intervention with AZM198 stabilized unstable plaque in the 0.4 mm segment proximal to the proximal suture, as assessed by the significant increase in cap thickness and cap area-to-lesion height ratio (Fig. 5C–E). Plaque stabilization by AZM198 was observed without changes to the lesion content of MPO protein (Fig. 5F) whereas Cl-Tyr, a marker of MPO activity, was decreased significantly by long-term treatment, but not short-term, with the MPO inhibitor (Fig. 5G). Analysis of AZM198 in plasma confirmed the absence of the MPO inhibitor two weeks after the drug was removed from the diet in the short-term treatment group, whereas the drug remained present in plasma in the long-term treatment group (Supplementary Fig. 3).

Plaque stabilization by AZM198 was observed without changes to

arterial staining of CD68 and Ly6B.2 (Fig. 6A–C), intraplaque measures of hemorrhage (Fig. 6A, D–E), and the lesion area under the cap (Fig. 6F). The importance of MPO in plaque destabilization was supported by correlation studies showing that plaque MPO protein, rather than CD68⁺- and Ly6B.2⁺-cells *per se*, correlated negatively with measures of cap thickness (Supplementary Fig. 4).

4. Discussion

Attenuating plaque destabilization by decreasing arterial inflammation is a potential novel treatment option to reduce the residual inflammatory risk present in up to one third of patients with cardiovascular disease despite their receiving optimal medical therapy and achieving low-density lipoprotein-cholesterol reduction [33]. Using a preclinical model of plaque instability, the present study shows that pharmacological inhibition of the pro-inflammatory enzyme MPO can stabilize existing unstable plaque. Our findings have translation potential for the treatment of high risk atherosclerosis, as the inhibitor used in the present study is a 2-thioxanthine, a class of irreversible suicide MPO inhibitor [19] that has successfully undergone Phase I studies in healthy subjects, and is in development for the treatment of heart failure with preserved ejection fraction [34,35].

Our findings are based on initiating the pharmacological inhibition of MPO when unstable plaque is already present, as verified by the characteristics of cap thinning, inflammatory cell infiltrates, cholesterol clefts and intraplaque hemorrhage. Comparing these features at the time of commencing the pharmacological intervention, *i.e.*, two weeks after TS surgery, with the time point characterized originally for the presence of unstable plaque, *i.e.*, seven weeks after TS surgery [17], revealed no substantial differences within the proximal 0.4 mm arterial segment. Therefore, two weeks after TS surgery is a suitable time point to commence intervention studies, and the proximal 0.4 mm arterial segment represents an appropriate location to assess intervention efficacy in this model of plaque instability.

The model has been used previously to probe the therapeutic potential of a statin [17], AZM198 [18], and sodium glucose co-transporter 2 (SGLT2) [36]. In those studies, therapy was initiated before or three days after TS surgery, *i.e.*, before unstable plaque was present (Figs. 3 and 4). Hence, those studies did not directly assess the ability of the therapeutic agents tested to stabilize existing unstable plaque. In contrast, and akin to the situation of a secondary prevention study in humans with established high-risk plaque, the present study for the first time tested the therapeutic efficacy of MPO inhibition commenced after unstable plaque had formed. Efficacy of plaque stabilization was verified by histological assessment of cap thickness as a primary measure because cap thickness and the cap area-to-lesion height ratio are well-established parameters that differentiate stable from unstable plaque prone to rupture [37]. Efficacy of MPO inhibition was verified by non-invasive molecular imaging of MPO activity, using the MRI agent MPO-Gd. MPO-Gd specifically detects MPO activity [38] and this has been validated for arterial MPO in the TS model of plaque instability [18]. While MPO-Gd relies on MRI, the advent of an activatable positron

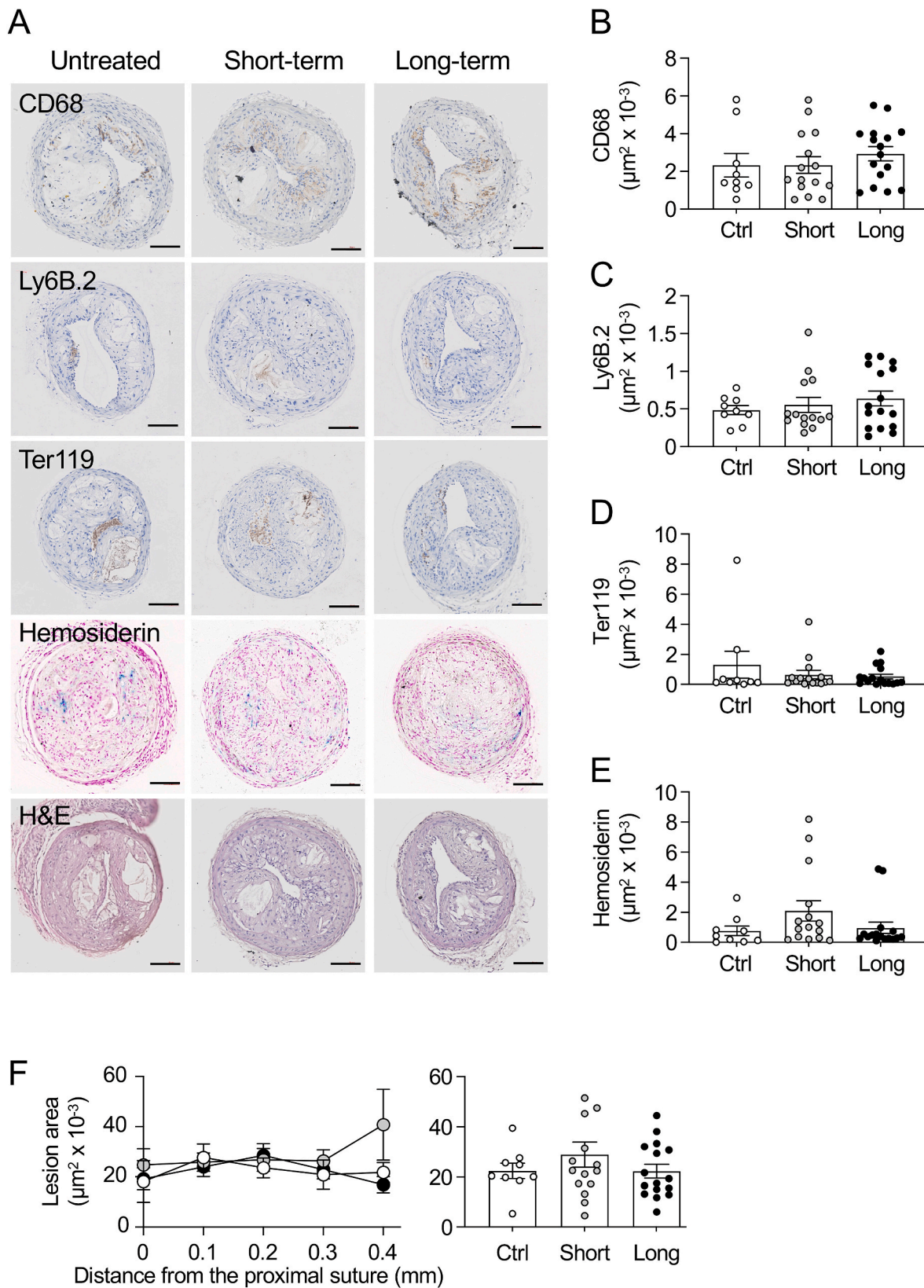


Fig. 6. Pharmacological inhibition of arterial MPO activity does not change the inflammatory cell content with the unstable plaque. (A) Representative images of sections of the right carotid artery 0–0.4 mm proximal to the proximal suture determined seven weeks after TS surgery from the short- and long-term MPO inhibition cohorts and stained for CD68, Ly6B.2, Ter119 or hemosiderin. (B–E) Average of areas stained positively for CD68, Ly6B.2, Ter119 or hemosiderin within the 0–0.4 mm region proximal to the proximal suture. H&E-stained images are included for comparison. (F) Lesion area under the fibrous cap in the 0–0.4 mm segment proximal to the proximal suture in untreated animals (open circles), short-term (grey circles) and long-term MPO inhibition cohorts (black circles) determined seven weeks after TS surgery (left panels), with data also expressed as averages (right panels). Data shows mean \pm SEM with $n = 9, 15$ and 16 for the untreated, short-term, and long-term groups, respectively.

emission tomography imaging radiotracer to report MPO activity *in vivo* [39] has the potential to facilitate the translation of non-invasive monitoring of MPO activity and inflammation in patients with cardiovascular disease and residual inflammation.

A key finding of the present study is that short-term intervention with the MPO inhibitor stabilized vulnerable plaque just as effectively as longer-term therapy (Fig. 5). This is of potential translational importance as anti-inflammatory therapies that improve cardiovascular disease outcome are limited and there are concerns about their potential to increase non-cardiovascular events [21–24]. Strikingly, we observed maintenance of plaque stability by short-term treatment with AZM198 even when assessed four weeks after cessation of MPO inhibitor therapy and at a time where arterial MPO activity increased to pre-inhibition levels. This may be explained by the fact that assessment of plaque stabilization by necessity was carried out within the proximal 0.4 mm region where unstable plaque was present prior to drug treatment, whereas the molecular MRI protocol determined MPO activity as a mean value over a comparatively longer, 3 mm region. In any case, the observed return to elevated arterial MPO activity following withdrawal of the MPO inhibitor, indicates the presence of sustained arterial inflammation in the TS model of plaque instability, in addition to its sustained systemic inflammation [32].

Whether and if so, how our findings relate to the human situation remains to be established. However, we can speculate on how the model's seven weeks period for the development of unstable atherosclerotic plaque, and the one week treatment with the MPO inhibitor, compare to human disease: a period of seven weeks in adult mice corresponds to ~18.8 human years [40], *i.e.*, a period sufficient for significant atherosclerosis including unstable plaque to develop in humans. A treatment period of one week in mice would correspond to a treatment period of 2.7 years in humans, *i.e.*, comparable to the median 3.7 year treatment with the therapeutic monoclonal antibody canakinumab targeting interleukin-1 β [21].

There may be concerns regarding potential side effects of MPO inhibition resulting from compromising the innate immune response, given the experience with anti-inflammatory therapies. Thus, therapeutic canakinumab is associated with a higher incidence of fatal infection [21] and low-dose colchicine in patients with recent myocardial infarction or chronic coronary disease is associated with more non-cardiovascular deaths that counterbalance the fewer cardiovascular deaths [24]. The present study did not address this issue, although AZM198 was used at a dose aimed to inhibit extracellular MPO activity by ~90% with limited inhibition of intracellular MPO activity [28] which is primarily responsible for MPO's role in innate immunity. Long-term human studies with MPO inhibitors have not been carried out to date. In phase I studies, once-daily single, and multiple ascending dosing of AZD4831 (a 2-thioxanthine-based MPO inhibitor like AZM198) in healthy volunteers was generally well tolerated [20]. From a clinical perspective, most patients with MPO deficiency are asymptomatic, with severe (candida) infectious complications occurring only occasionally in the setting of comorbid diabetes mellitus. Therefore, partial, and selective inhibition of extracellular MPO activity may be a suitable pharmacological strategy to treat high-risk atherosclerosis without compromising innate immune defenses seen with other anti-inflammatory drugs.

Our findings also highlight a remarkable dynamic responsiveness of non-invasive molecular MRI of MPO activity in response to onset and withdrawal of pharmacological MPO inhibition. In addition, our results reveal a high level of reproducibility obtained with MPO-Gd between different studies, and the ability of this method to carry out longitudinal analyses of individual animals. This ability for reliable tracer detection opens the opportunity to perform meaningful longitudinal studies without the need for large animal numbers. A disadvantage of molecular MRI is cost, and relevant equipment may not be readily available. *In vivo* molecular MRI provides a direct measure of MPO activity present at the time of analysis, whereas immunohistochemical determination of Cl-

Tyr, a product of MPO activity, reflects the time-dependent formation and removal/metabolism of Cl-Tyr. As such, the latter does not reflect actual MPO activity at the time of tissue collection. As neither the rate of formation of Cl-Tyr nor its turnover are known, it is conceivable that the time-dependent changes to Cl-Tyr do not precisely reflect the time-dependent changes to MPO activity, and this may help explain why short-term treatment with AZM198 did not decrease plaque Cl-Tyr content.

Although recognized as an important contributor, plaque destabilization itself does not solely cause acute cardiovascular events. Therefore, it will be important to establish whether and if so how, pharmacological inhibition of arterial MPO activity alleviates plaque rupture and ensuing thrombosis. We are currently addressing this question in a rabbit model of plaque rupture/thrombosis [41], just as preliminary studies indicate that elevated MPO activity is also a characteristic feature of unstable human carotid and coronary plaque. The present study only employed male mice, *i.e.*, the sex in which the TS mouse model was developed [17]. However, male and female mice may respond differently to surgery and treatment, so that it will be important to establish whether the findings of the present study extend to female mice.

Overall, these observations, together with the successful phase I studies with 2-thioxanthine-based MPO inhibitor [34,35], indicate that inhibition of MPO activity may represent a useful therapeutic approach to attenuate arterial inflammation in patients with high-risk atherosclerotic disease.

Funding

This work was supported by National Health and Medical Research Council of Australia Program Grant APP1052616 and Senior Principal Research Fellowship APP1111632, as well as NSW Health, Australia Senior Scientist Grant to R.S.

Declaration of competing interest

ED is an AstraZeneca employee and holds shares in AstraZeneca, which is developing the myeloperoxidase inhibitor AZD4831 for the treatment of HFpEF. RS has received in-kind support from AstraZeneca. All other authors declare that they have no known competing financial interests or personal relationships that could have appeared to influence the work reported in this paper.

Data availability

Data will be made available on request.

Acknowledgements

We acknowledge the technical support from Mr Darren Newington and Dr Jihan Talib (Victor Chang Cardiac Research Institute), Mr Brendan Lee (UNSW), Dr Yunjia Zhang (UNSW), Dr James Nadel (HRI) and Dr Sián Cartland (Heart Research Institute). We thank Dr Imran Rashid (University Hospitals Cleveland Medical Center) for critically reading the manuscript, and acknowledge the facilities and scientific and technical assistance of the National Imaging Facility, a National Collaborative Research Infrastructure Strategy (NCRIS) capability, at the Biological Resource Imaging Laboratory, UNSW.

Appendix A. Supplementary data

Supplementary data to this article can be found online at <https://doi.org/10.1016/j.redox.2022.102532>.

References

- [1] P. Libby, History of discovery: inflammation in atherosclerosis, *Arterioscler. Thromb. Vasc. Biol.* 32 (2012) 2045–2051.
- [2] H. Parker, A.M. Albrett, A.J. Kettle, C.C. Winterbourn, Myeloperoxidase associated with neutrophil extracellular traps is active and mediates bacterial killing in the presence of hydrogen peroxide, *J. Leukoc. Biol.* 91 (2012) 369–376.
- [3] N. Teng, G.J. Maghzal, J. Talib, I. Rashid, A.K. Lau, R. Stocker, The roles of myeloperoxidase in coronary artery disease and its potential implication in plaque rupture, *Redox Rep.* 22 (2017) 51–73.
- [4] T. Naruko, M. Ueda, K. Haze, A.C. van der Wal, C.M. van der Loos, A. Itoh, R. Komatsu, Y. Ikura, M. Ogami, Y. Shimada, S. Ehara, M. Yoshiyama, K. Takeuchi, J. Yoshikawa, A.E. Becker, Neutrophil infiltration of culprit lesions in acute coronary syndromes, *Circulation* 106 (2002) 2894–2900.
- [5] G. Ferrante, M. Nakano, F. Prati, G. Niccoli, M.T. Mallus, V. Ramazzotti, R. A. Montone, F.D. Kolodgie, R. Virmani, F. Crea, High levels of systemic myeloperoxidase are associated with coronary plaque erosion in patients with acute coronary syndromes: a clinicopathological study, *Circulation* 122 (2010) 2505–2513.
- [6] M.G. Ionita, P. van den Borne, L.M. Catanzariti, F.L. Moll, J.P. de Vries, G. Pasterkamp, A. Vink, D.P. de Kleijn, High neutrophil numbers in human carotid atherosclerotic plaques are associated with characteristics of rupture-prone lesions, *Arterioscler. Thromb. Vasc. Biol.* 30 (2010) 1842–1848.
- [7] A. Daugherty, J.L. Dunn, D.L. Rateri, J.W. Heinecke, Myeloperoxidase, a catalyst for lipoprotein oxidation, is expressed in human atherosclerotic lesions, *J. Clin. Invest.* 94 (1994) 437–444.
- [8] L.J. Hazell, L. Arnold, D. Flowers, G. Waeg, E. Malle, R. Stocker, Presence of hypochlorite-modified proteins in human atherosclerotic lesions, *J. Clin. Invest.* 97 (1996) 1535–1544.
- [9] S. Sugiyama, Y. Okada, G.K. Sukhova, R. Virmani, J.W. Heinecke, P. Libby, Macrophage myeloperoxidase regulation by granulocyte macrophage colony-stimulating factor in human atherosclerosis and implications in acute coronary syndromes, *Am. J. Pathol.* 158 (2001) 879–891.
- [10] R.J. Roth Flach, C. Su, E. Bollinger, C. Cortes, A.W. Robertson, A.C. Opsahl, T. M. Coskran, K.P. Maresca, E.J. Keliher, P.D. Yates, A.M. Kim, A.S. Kalgutkar, L. Buckbinder, Myeloperoxidase inhibition in mice alters atherosclerotic lesion composition, *PLoS One* 14 (2019), e0214150.
- [11] M.L. Brennan, M.M. Anderson, D.M. Shih, X.D. Qu, X. Wang, A.C. Mehta, L.L. Lim, W. Shi, S.L. Hazen, J.S. Jacob, J.R. Crowley, J.W. Heinecke, A.J. Lusis, Increased atherosclerosis in myeloperoxidase-deficient mice, *J. Clin. Invest.* 107 (2001) 419–430.
- [12] V. Tiyerili, B. Camara, M.U. Becher, J.W. Schrickel, D. Lütjohann, M. Mollenhauer, S. Baldus, G. Nickenig, R.P. Andrié, Neutrophil-derived myeloperoxidase promotes atherogenesis and neointima formation in mice, *Int. J. Cardiol.* 204 (2016) 29–36.
- [13] B. Bathish, R. Turner, M. Paumann-Page, A.J. Kettle, C.C. Winterbourn, Characterisation of peroxidase activity in isolated extracellular matrix and direct detection of hypobromous acid formation, *Arch. Biochem. Biophys.* 646 (2018) 120–127.
- [14] L.V. Forbes, A.J. Kettle, A multi-substrate assay for finding physiologically effective inhibitors of myeloperoxidase, *Anal. Biochem.* 544 (2018) 13–21.
- [15] R. Virmani, F.D. Kolodgie, A.P. Burke, A. Farb, S.M. Schwartz, Lessons from sudden coronary death: a comprehensive morphological classification scheme for atherosclerotic lesions, *Arterioscler. Thromb. Vasc. Biol.* 20 (2000) 1262–1275.
- [16] J. Nadel, A. Jabbour, R. Stocker, Arterial myeloperoxidase in the detection and treatment of vulnerable atherosclerotic plaque: a new dawn for an old light, *Cardiovasc. Res.* (2022), <https://doi.org/10.1093/cvr/cvac081>. May 19;cvac081.
- [17] Y.C. Chen, A.V. Bui, J. Diesch, R. Manasseh, C. Hausding, J. Rivera, I. Haviv, A. Agrotis, N.M. Htun, J. Jowett, C.E. Hagemeyer, R.D. Hannan, A. Bobik, K. Peter, A novel mouse model of atherosclerotic plaque instability for drug testing and mechanistic/therapeutic discoveries using gene and microRNA expression profiling, *Circ. Res.* 113 (2013) 252–265.
- [18] I. Rashid, G.J. Maghzal, Y.C. Chen, D. Cheng, J. Talib, D. Newington, M. Ren, S. K. Vajandar, A. Searle, A. Maluenda, E.L. Lindstedt, A. Jabbour, A.J. Kettle, A. Bongers, C. Power, E. Michaëlsson, K. Peter, R. Stocker, Myeloperoxidase is a potential molecular imaging and therapeutic target for the identification and stabilization of high-risk atherosclerotic plaque, *Eur. Heart J.* 39 (2018) 3301–3310.
- [19] A.K. Tiden, T. Sjogren, M. Svensson, A. Bernlind, R. Senthilmohan, F. Auchere, H. Norman, P.O. Markgren, S. Gustavsson, S. Schmidt, S. Lundquist, L.V. Forbes, N. J. Magon, L.N. Paton, G.N. Jameson, H. Eriksson, A.J. Kettle, 2-Thioxanthines are mechanism-based inactivators of myeloperoxidase that block oxidative stress during inflammation, *J. Biol. Chem.* 286 (2011) 37578–37589.
- [20] T. Inghardt, T. Antonsson, C. Ericsson, D. Hovdal, P. Johannesson, C. Johannsson, U. Jurva, J. Kajanus, B. Kull, E. Michaëlsson, A. Pettersen, T. Sjogren, H.K. W. Sorensen, E.-L. Lindstedt, Discovery of AZD4831, a mechanism-based irreversible inhibitor of myeloperoxidase, as a potential treatment for heart failure with preserved ejection fraction, *J. Med. Chem.* 65 (2022) 11485–11496.
- [21] P.M. Ridker, B.M. Everett, T. Thuren, J.G. MacFadyen, W.H. Chang, C. Ballantyne, F. Fonseca, J. Nicolau, W. Koenig, S.D. Anker, J.J.P. Kastelein, J.H. Cornel, P. Pais, D. Pella, J. Genest, R. Cifkova, A. Lorenzatti, T. Forster, Z. Kobalava, L. Vida-Simiti, M. Flather, H. Shimokawa, H. Ogawa, M. Dellborg, P.R.F. Rossi, R.P.T. Troquay, P. Libby, R.J. Glynn, C.T. Group, Antiinflammatory therapy with Canakinumab for atherosclerotic disease, *N. Engl. J. Med.* 377 (2017) 1119–1131.
- [22] P.M. Ridker, B.M. Everett, A. Pradhan, J.G. MacFadyen, D.H. Solomon, E. Zaharris, V. Mam, A. Hasan, Y. Rosenberg, E. Iturriaga, Low-dose methotrexate for the prevention of atherosclerotic events, *N. Engl. J. Med.* 380 (2019) 752–762.
- [23] K. Broch, A.K. Anstensrud, S. Woxholt, K. Sharma, I.M. Tollefsen, B. Bendz, S. Aakhus, T. Ueland, B.H. Amundsen, J.K. Damàs, Randomized trial of interleukin-6 receptor inhibition in patients with acute ST-segment elevation myocardial infarction, *J. Am. Coll. Cardiol.* 77 (2021) 1845–1855.
- [24] A.T.L. Fiolet, T.S.J. Opstal, A. Mosterd, J.W. Eikelboom, S.S. Jolly, A.C. Keech, P. Kelly, D.C. Tong, J. Layland, S.M. Nidorf, P.L. Thompson, C. Budgeon, J.G. P. Tijssen, J.H. Cornel, Efficacy and safety of low-dose colchicine in patients with coronary disease: a systematic review and meta-analysis of randomized trials, *Eur. Heart J.* 42 (2021) 2765–2775.
- [25] F. Tang, X.D. Manz, A. Bongers, R.A. Odell, H. Joukhdar, J.M. Whitelock, M. S. Lord, J. Rnjak-Kovacina, Microchannels are an architectural cue that promotes integration and vascularization of silk biomaterials in vivo, *ACS Biomater. Sci. Eng.* 6 (2020) 1476–1486.
- [26] J.W. Chen, M. Querol Sans, A. Bogdanov Jr., R. Weissleder, Imaging of myeloperoxidase in mice by using novel amplifiable paramagnetic substrates, *Radiology* 240 (2006) 473–481.
- [27] B. Pulli, M. Ali, R. Forghani, S. Schob, K.L.C. Hsieh, G. Wojtkiewicz, J. Linnoila Jr., J.W. Chen, Measuring myeloperoxidase activity in biological samples, *PLoS One* 8 (2013), e67976.
- [28] H. Björnsdóttir, A. Welin, E. Michaëlsson, V. Osla, S. Berg, K. Christenson, M. Sundqvist, C. Dahlgren, A. Karlsson, J. Bylund, Neutrophil NET formation is regulated from the inside by myeloperoxidase-processed reactive oxygen species, *Free Radic. Biol. Med.* 89 (2015) 1024–1035.
- [29] W. Chen, S. Tumanov, D. Fazarkeley, J. Cantley, D.E. James, L.L. Dunn, T. Shaik, C. Suarna, R. Stocker, Bilirubin deficiency renders mice susceptible to hepatic steatosis in the absence of insulin resistance, *Redox Biol.* (2021).
- [30] L.L. Dunn, S.M.Y. Kong, S. Tumanov, W. Chen, J. Cantley, A. Ayer, G.J. Maghzal, R. G. Midwinter, K.H. Chan, M.K.C. Ng, R. Stocker, Hmox1 (heme oxygenase-1) protects against ischemia-mediated injury via stabilization of HIF-1 α (hypoxia-inducible factor-1 α), *Arterioscler. Thromb. Vasc. Biol.* 41 (2021) 317–330.
- [31] J.S. Gujral, J.A. Hinson, A. Farhood, H. Jaeschke, NADPH oxidase-derived oxidant stress is critical for neutrophil cytotoxicity during endotoxemia, *Am. J. Physiol. Gastrointest. Liver Physiol.* 287 (2004) G243–G252.
- [32] D. Cheng, J. Talib, C.P. Stanley, I. Rashid, E. Michaëlsson, E.L. Lindstedt, K. D. Croft, A.J. Kettle, G. Maghzal, R. Stocker, Inhibition of myeloperoxidase attenuates endothelial dysfunction in mouse models of vascular inflammation and atherosclerosis, *Arterioscler. Thromb. Vasc. Biol.* 39 (2019) 1448–1457.
- [33] O. Bayturan, S. Kapadia, S.J. Nicholls, E.M. Tuzcu, M. Shao, K. Uno, A. Shreevatsa, A.J. Lavoie, K. Wolksi, P. Schoenhagen, Clinical predictors of plaque progression despite very low levels of low-density lipoprotein cholesterol, *J. Am. Coll. Cardiol.* 55 (2010) 2736–2742.
- [34] L.M. Gan, M. Lagerström-Fermér, H. Ericsson, K. Nelander, E.L. Lindstedt, E. Michaëlsson, M. Kjaer, M. Heijer, C. Whatling, R. Fuhr, Safety, tolerability, pharmacokinetics and effect on serum uric acid of the myeloperoxidase inhibitor AZD4831 in a randomized, placebo-controlled, phase I study in healthy volunteers, *Br. J. Clin. Pharmacol.* 85 (2019) 762–770.
- [35] K. Nelander, M. Lagerström-Fermér, C. Amilon, E. Michaëlsson, M. Heijer, M. Kjaer, M. Russell, D. Han, E.L. Lindstedt, C. Whatling, L.M. Gan, H. Ericsson, Early clinical experience with AZD4831, a novel myeloperoxidase inhibitor, developed for patients with heart failure with preserved ejection fraction, *Clin. Transl. Sci.* 14 (2021) 812–819.
- [36] Y.C. Chen, K. Jandeleit-Dahm, K. Peter, Sodium-glucose co-transporter 2 (SGLT2) inhibitor dapagliflozin stabilizes diabetes-induced atherosclerotic plaque instability, *J. Am. Heart Assoc.* 10 (2021), e022761.
- [37] J.N. Redgrave, P. Gallagher, J.K. Lovett, P.M. Rothwell, Critical cap thickness and rupture in symptomatic carotid plaques. The Oxford plaque study, *Stroke* 39 (2008) 1722–1729.
- [38] M. Nahrendorf, D. Sosnovik, J.W. Chen, P. Panizzi, J.L. Figueiredo, E. Aikawa, P. Libby, F.K. Swirski, R. Weissleder, Activatable magnetic resonance imaging agent reports myeloperoxidase activity in healing infarcts and noninvasively detects the antiinflammatory effects of atorvastatin on ischemia-reperfusion injury, *Circulation* 117 (2008) 1153–1160.
- [39] C. Wang, E. Keliher, M.W.G. Zeller, G.R. Wojtkiewicz, A.D. Aguirre, L. Buckbinder, H.-Y. Kim, J. Chen, K. Maresca, M.S. Ahmed, N. Jalali Motlagh, M. Nahrendorf, J. W. Chen, An activatable PET imaging radioprobe is a dynamic reporter of myeloperoxidase activity in vivo, *Proc. Natl. Acad. Sci. U.S.A.* 116 (2019) 11966–11971.
- [40] S. Dutta, P. Sengupta, Men and mice: relating their ages, *Life Sci.* 152 (2016) 244–248.
- [41] A. Phinikaridou, K.J. Hallock, Y. Qiao, J.A. Hamilton, A robust rabbit model of human atherosclerosis and atherothrombosis, *J. Lipid Res.* 50 (2009) 787–797.